



LAWRENCE  
LIVERMORE  
NATIONAL  
LABORATORY

# Experimental and Theoretical Measurements of Concentration Distributions in Acoustic Focusing Devices

K. A. Rose, K. Fisher, B. Jung, K. Ness, R. P.  
Mariella Jr.

June 23, 2008

Micro Total Analysis Systems  
San Diego, CA, United States  
October 12, 2008 through October 16, 2008

## **Disclaimer**

---

This document was prepared as an account of work sponsored by an agency of the United States government. Neither the United States government nor Lawrence Livermore National Security, LLC, nor any of their employees makes any warranty, expressed or implied, or assumes any legal liability or responsibility for the accuracy, completeness, or usefulness of any information, apparatus, product, or process disclosed, or represents that its use would not infringe privately owned rights. Reference herein to any specific commercial product, process, or service by trade name, trademark, manufacturer, or otherwise does not necessarily constitute or imply its endorsement, recommendation, or favoring by the United States government or Lawrence Livermore National Security, LLC. The views and opinions of authors expressed herein do not necessarily state or reflect those of the United States government or Lawrence Livermore National Security, LLC, and shall not be used for advertising or product endorsement purposes.

# EXPERIMENTAL AND THEORETICAL MEASUREMENTS OF CONCENTRATION DISTRIBUTIONS IN ACOUSTIC FOCUSING DEVICES

Klint A. Rose, Karl Fisher, Byoungsok Jung, Kevin Ness, and  
Raymond P. Mariella Jr.

Lawrence Livermore National Laboratory, USA

## ABSTRACT

We describe a modeling approach to capture the particle motion within an acoustic focusing microfluidic device. Our approach combines finite element models for the acoustic forces with analytical models for the fluid motion and uses these force fields to calculate the particle motion in a Brownian dynamics simulation. We compare results for the model with experimental measurements of the focusing efficiency within a microfabricated device. The results show good qualitative agreement over a range of acoustic driving voltages and particle sizes.

**KEYWORDS:** Acoustic focusing, Brownian dynamics, modeling, sample prep

## INTRODUCTION

Acoustic focusing is an effective technique to manipulate relatively large particles ( $> 2 \mu\text{m}$ ) and has been used for a variety of applications including sorting blood cells [1], concentrating cells for optical detection [2], and measuring particle zeta potentials [3]. We are currently investigating acoustic focusing in microchannels for removing cells, pollen, and other large contaminants from human nasopharyngeal samples as a front-end preparation step before viral identification assays. By focusing large contaminants into a single plane or node within the microchannel, we can separate a complex input sample into waste and purified streams and direct each to separate outputs.

## THEORY

The location and width of the focused particle band depend on the channel geometry, material properties, and acoustic transducer operating conditions. The transducer generates pressure fields within the microchannel (Figure 1) creating acoustic radiation forces whose direction and magnitude depend on the relative compressibility and density of the particle and the fluid [4]. Currently, models predicting net particle motion within acoustically driven devices rely on simplified 1-D models for the acoustic forces [5]. Fisher et al. used FEM simulations to analyze the 2-D force field in a microfluidic device, but this analysis only provides qualitative information regarding the likely particle locations [6].

In our approach, we solve for the hydrodynamic flow field using analytical solutions based on the geometry of the microchannel and solve for the two-dimensional acoustic force field within the channel using a commercial FEM code (ATILA FEA). We incorporate the force fields into a Brownian dynamics simulation based on the

Langevin equation. This simulation includes random displacements due to Brownian motion and calculates spatial and temporal concentration distributions for any species within the device.

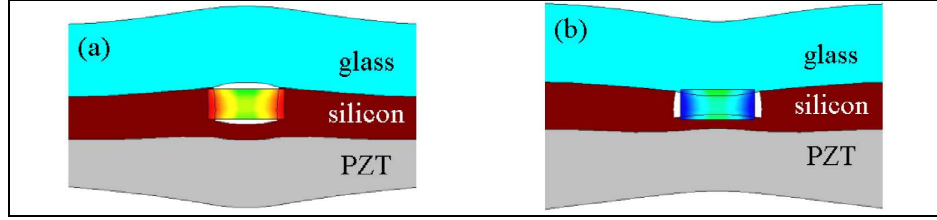


Figure 1. Example of the pressure fields generated in a fluid volume (fixed rectangular center) by a glass-silicon-PZT stack. (a) High pressures (red) generated at the edges of the fluid volume as the sidewalls compress inward. (b) Low pressures (blue) generated at fluid volume edges as the sidewalls expand outward.

## EXPERIMENTAL

To validate the model we experimentally measured the degree of focusing (full width half maximum) for microspheres with diameters ranging from 1 to 5  $\mu\text{m}$  (Invitrogen; Carlsbad, CA). We used a microfluidic chip, shown in Figure 2, with channels etched into a silicon wafer and a PZT glued to the backside.

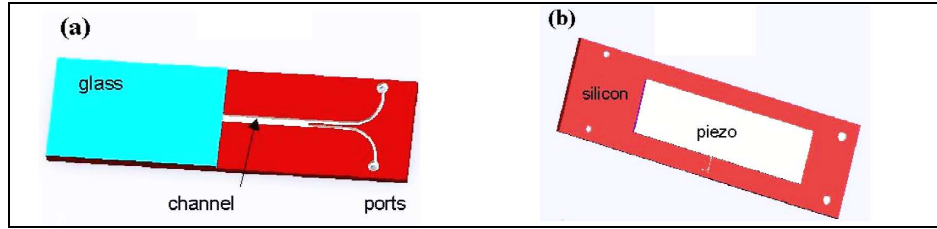


Figure 2. CAD drawing of the microfluidic chip used to validate the simulation. (a) Front view of chip showing the glass top and bifurcated separation channel etched into the silicon base. (b) Bottom view of the chip showing the PZT.

We operated the PZT at a frequency of 1.46 MHz and varied the input voltage from 0 to 9.6 V. We maintained the input flow rate for the particle-laden aqueous solution at 10  $\mu\text{L}/\text{min}$ . The 2-D force field we predicted for these conditions (Figure 3) suggests a single node in the lower center region of the channel. The experimental data points were calculated by averaging over ten 1392 by 312 pixel CCD images near the outlet of the microchannel.

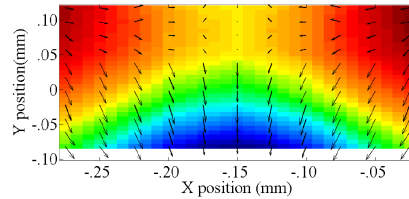


Figure 3. Simulated result for the acoustic radiation force field in the microfluidic chip cross-section when the PZT is driven at 1.46 MHz. The colormap indicates the high (red) to low (blue) pressure field. Arrows show the direction of the acoustic forces.

## RESULTS AND DISCUSSION

The experimental and simulated results for the width of the resulting focused particle band, shown in Figure 4, compare favorably across particle sizes and driving voltages when the simulated values are scaled by a factor of 40. This result demonstrates our ability to qualitatively capture the acoustic focusing force magnitudes and directions versus the input flow rates and random particle motion. Our future work will aim to eliminate the need for a scaling factor by modeling the full 3-D force field and including losses due to material interfaces.

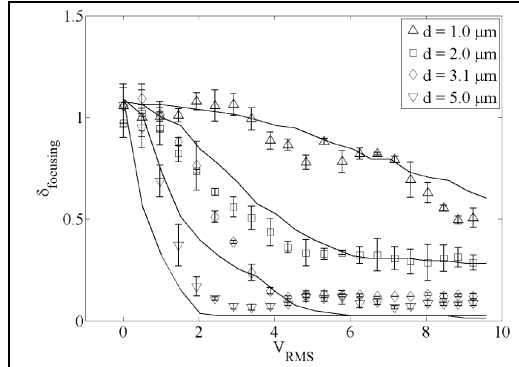


Figure 3. Comparison of experimental and theoretical measurements. The solid lines show the theoretical force field predicted from the simulations and the symbols indicate the experimental values.

## CONCLUSIONS

Using the methodology described here, we can rapidly iterate over a variety of input parameters including geometry, acoustic driving voltage and frequency, and particle properties to predict the spatial and temporal particle concentration distributions within a microfluidic device and achieve an optimized design.

## ACKNOWLEDGEMENTS

This work was performed under the auspices of the U.S. Department of Energy by Lawrence Livermore National Laboratory under Contract DE-AC52-07NA27344.

## REFERENCES

- [1] Kapishnikov, S., V. Kantsler and V. Steinberg, *Continuous particle size separation and size sorting using ultrasound in a microchannel*, Journal of Statistical Mechanics, 2006, P01012.
- [2] Zhou, C., P. Pivarnik, A.G. Rand, S.V. Letcher, *Acoustic standing-wave enhancement of a fiber-optic Salmonella biosensor*, Biosensors & Bioelectronics, 1998, 13, p. 495–500
- [3] Hunter, R.J. and R.W. O'Brien, *Electroacoustic Characterization of Colloids with Unusual Particle Properties*. Colloids and Surfaces A: Physicochemical and Engineering Aspects, 1997. 126: p. 123-128.
- [4] Nyborg, W.L., *Radiation Pressure on a Small Rigid Sphere*, Journal of the Acoustical Society of America, 1967, 42:5, p. 947
- [5] Martyn H., Y. Shen, and J.J. Hawkes, *Modeling of layered resonators for ultrasonic separation*, Ultrasonics, 2002, 40, p. 385–392.
- [6] Fisher, K., Miles, R., *Modeling Acoustic Radiation Forces in MicroFluidic Chambers*, Journal of the Acoustical Society of America 2008, 123, 1100-1104.